Networks and Heterogeneous Media

https://www.aimspress.com/journal/nhm

NHM, 19(1): 384–404.
DOI: 10.3934/nhm.2024017
Received: 16 May 2023
Revised: 18 December 2023
Accepted: 29 December 2023
Published: 04 April 2024

Research article

Mean time to infection by small diffusing droplets containing SARS-CoV-2 during close social contacts

U. Dobramysl[1], **C. Sieben**[2] **and D. Holcman**[3,*]

[1] Peter Medawar Building for Pathogen Research, Nuffield Department of Medicine, University of Oxford, Oxford, UK

[2] Nanoscale Infection Biology Group, Helmholtz Centre for Infection Research, 38124 Braunschweig, Germany

[3] Group of data modeling and computational biology, IBENS-PSL Ecole Normale Superieure, Paris, France

* **Correspondence:** Email: david.holcman@ens.fr.

Abstract: Airborne viruses such as SARS-CoV-2 are partly spread through aerosols containing viral particles. Inhalation of infectious airborne particles can lead to infection, a route that can be even more predominant than droplet or contact transmission. To study the transmission between a susceptible and an infected person, we estimated the distribution of arrival times of small diffusing aerosol particles to the inhaled region located below the nose until the number of particles reaches a critical threshold. Our results suggested that although contamination by continuous respiration can take approximately 90 min at a distance of 0.5 m, it is reduced to a few minutes when coughing or sneezing. Interestingly, there is not much difference between outdoors and indoors when the air is still. When a window is open inside an office, the infection time is reduced. Finally, wearing a mask leads to a delay in the time to infection. To conclude, diffusion analysis provides several key timescales of viral airborne transmission.

Keywords: aerosol diffusion; mean time to infection; simulations; modeling; SARS-CoV-2

1. Introduction

Airborne SARS-CoV-2 viruses spread between humans in particular through respiratory droplets [14, 17] expelled during breathing, coughing or sneezing from an infectious person. Droplets resulting from coughing or sneezing can infect a target person by entering into the respiratory mucosa. These droplets can be separated in coarse (>5 μm) and fine ($\leq$ 5 μm) fractions. Although large particles can be respired and reach alveolar tissues [7], they usually fall to the ground quickly

within 1–2 m [28, 29]. However, smaller droplets (aerosols) remain suspended in the air for much longer periods of time, having been found to be infectious even after 12 h [15]. This route most likely leads to major spreading at home, work, hospitals and in urgent care medical units [20]. Indeed, indoor space is a major SARS-CoV-2 infection risk [20], as the virus can be transmitted via speech droplets [3]. Aerosol particles are able to travel hundreds of meters or more [31]. Furthermore, fine particles were found to contain 8.8 times more viral copies than coarse particles [18]. Yet, precisely quantifying the infectivity due to aerosols transmission remains difficult: it is hard to measure the droplets despite recent efforts [3], and the step from droplet dispersion to human contamination requires an assessment of the efficiency of infection. To get around these difficulties, data was obtained in ferrets [12], although it still remained difficult to extrapolate these aerosol transmission measurements to the human scale. In ferrets, sneezing increases the number of small droplets [12] and the majority of particles generated during sneezing were < 5 μm. For example, exhaled aerosol particles from infected or naive ferrets during normal breathing (for 30 min) or sneezing (for 5 min) both lead to around 5000 droplets produced. In influenza, human study participants exhaled between 3.2 and 20 virus RNA copies per minute [9], which is assumed to be of similar magnitude for SARS-CoV-2. The motion of aerosolized particles is well approximated as a diffusion process, with a size-dependent diffusion coefficient ranging from $D = 10^{-4}$ m^2/s, for a size around 0.1 μm to $D = 10^{-7}$ m^2/s, for 5 μm [25].

Here, we compute the time it takes for a susceptible person to get infected when in close proximity to an infected person. By susceptible, we assume that the person has not been exposed before and that their immune system is naive regarding the pathogen. We explore how this transmission depends on the number of viral particles, air transportation parameters and the distance between two persons. We adopt the terminology clinicians use for airborne infectious diseases throughout this paper, meaning that an aerosol or aerosolized particle refers to an airborne drop of liquid smaller than 10 μm and a particle is equivalent to a virion [27, 30]. Influenza A has a 50% human infectious dose (HID_50) of around 1000–2000 viral particles [1, 19, 32]. The HID_50 is not known for SARS-CoV-2, but medical experts estimate it to be lower than for Influenza A, between hundreds and thousands of viral particles [22, 23]. We therefore model infection by counting the number of viral particles a susceptible person inhaled until the threshold number for infection is reached. From the above, we set this threshold to be at 100 particles, the lowest reasonable number for SARS-CoV-2 (see Section 4.2). We estimate the probability and the mean time to infection (i.e., until the threshold is reached) when the infectious and susceptible person are placed in the same room or outside using diffusion modeling and numerical simulations of aerosols. We evaluate the role of wearing a mask [13] in several different scenarios, including regular respiration cycles (exhalation) and coughing. While surgical masks reduce viral copy numbers in the coarse droplet fraction by a factor of 25, we focus here on the fine fraction, where they reduce the viral aerosol load only by a factor of 2.8 [18]. Indeed, there are much more efficient masks or respirators available [10], but our aim is to show the effects for these simple masks. Finally, we explore the sensitivity of several key parameters such as the diffusion coefficient or the viral copy number threshold required for infection. In summary, we found that being in the same room as a non-coughing infectious person for less than 100 min does not lead to infection, while being exposed to a coughing person without protection can lead to infection within minutes. We did not investigate the time to infection when the infected person is talking, due to the variability in aerosolized particle production during speech [2, 4, 11] (however, we speculate that it would be similar to the coughing

case). We conclude that wearing a mask can strongly suppress the propagation of infection via the small aerosol particle route.

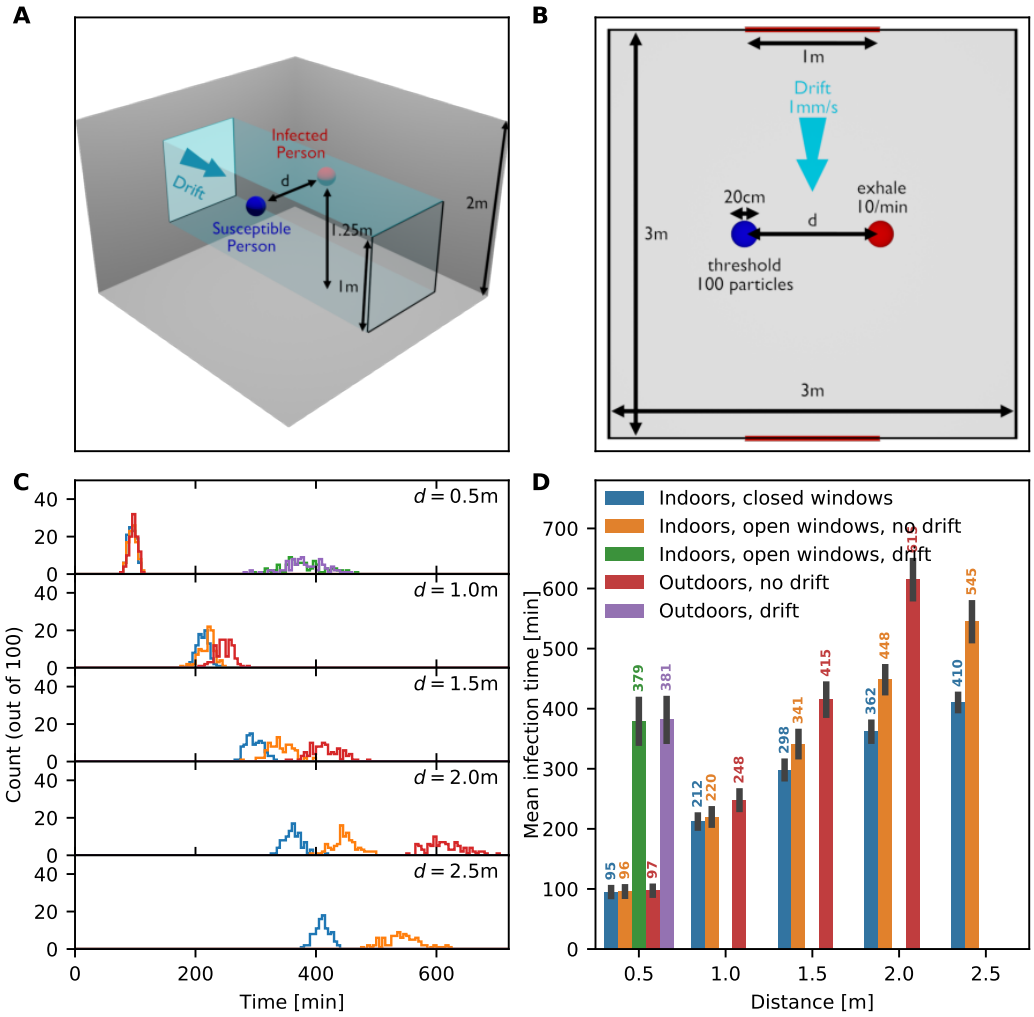

Figure 1. Simulations of infection by diffusing aerosols: infection time distribution when an infected person is breathing only. (a) 3D schematic representation of a closed room containing an infected (red) and a susceptible (blue) person separated by a variable distance d. The room contains two windows which can be either open or closed, and a possible drift of air between the windows. (b) 2D schematic projection of (a). Room and window dimensions are displayed in the schematics. (c) Distribution of time of infection for distances $d = 0.5, 1, 1.5, 2$ and 2.5 m and the following scenarios: indoors with windows closed (blue), indoors with open windows and no drift (orange), indoors with open windows and a drift (green), outdoors without drift (red), and outdoors with drift (purple). (d) Mean infection time for the different scenarios. Missing bars indicate scenarios in which at least one realization had an infection time beyond 12 h. Error bars indicate the standard deviation of the time distribution.

2. Results

2.1. Viral propagation by small diffusing aerosol particles: a diffusion modeling approach

We model viral diffusion and infection as follows: an infected person is positioned at a distance d from a susceptible person, either in a $3 \times 2 \times 2$ m room or outside (Figure 1a). We address the difference in the release of free diffusing aerosols during regular respiration (exhalation) and sneezing or coughing, by changing the initial distribution and increasing the number of droplets (see Section 4.1): coughing is modeled by releasing 10^4 viral particles instantaneously with a rate in a range between 30 s to 5 min [33]. Each viral particle is contained in their own aerosolized particle of 0.1 μm size [16, 33]. The full particle load is randomly and uniformly distributed in a sphere of 1 m diameter directly in front of the infected person's head.

We also investigated breathing without coughing (in e.g., asymptomatic cases). In this case, we use a production of 10 particles per minute at the location of the infected person's head. This value was motivated from Fabian et al., [9], who found between 3 and 20 viral RNA copies per minute in patients infected with influenza A, and from Milton et al., [18], who found a median of 560 viral RNA copies in 30 min of sampling. The susceptible person is modeled as an absorbing sphere of 10 cm radius around the person's head. This accounts for the breathed-in volume of air during inhalation.

Infection occurs when a threshold number of 100 viral particles are inhaled by the susceptible person, accounting for the fact that the independent action hypothesis likely does not hold for SARS-CoV-2 [26].

In the indoors case, the room has a pair of windows in the centers of the long walls (opposite each other) that can either be open or closed. When the windows are open (where they act as absorbing surfaces), there can be a small draft (resulting in a drift of 1 mm/s) in the volume between the windows or no draft. In the outdoors case, it is either wind-still, or the same drift is applied throughout the domain. In our simulations, these cases were differentiated by implementing different boundary conditions. Finally, the susceptible person can wear a mask, in which case only one in 2.8 particles is absorbed on average [18].

2.2. Aerosol infection due to breathing indoors and outdoors

We first study the time to infection based on diffusing aerosols in a closed room, containing a susceptible person separated by a distance d from an infected person (Figure 1a,b). We run simulations to obtain the distribution of infection times to reach a cumulative infection threshold $T = 100$ of aerosol particles inhaled by the susceptible person (using 100 realizations). As we vary the distance d (Figure 1c), we find that the mean time of infection increases drastically: For $d = 0.5, 1$, and 2 m, we found a mean time of 95 ± 7 min, 212 ± 10 min, and 362 ± 15 min (mean and standard deviation, respectively). Open windows alone, or even being outside, have no effect at small distances (for $d \leq 1$ m) and an increasing but still small effect at larger distances ($d \geq 1$ m) on these time scales (Figure 1c,d). A small drift of 1 mm/s perpendicular to the axis connecting the two persons leads to an increase of the time of infection to around 381 ± 35 min, a four-fold increase at a distance of $d = 0.5$ m. For larger distances, we do not show the infection time because it is beyond our simulation time limit of 12 h. Hence, in our model of diffusing aerosols generated by periodic breathing with 10 viral particles released per minute, we found that the infection threshold of 100 absorbed particles is reached in around 1.5 h.

Open windows without a drift does not change this timescale substantially, but ventilation in form of a drift does.

We derived the mathematical expression for the infection time as a function of distance (see Eq (4.11)). This provides a good fit to the simulation results for the outdoor case (Figure S4).

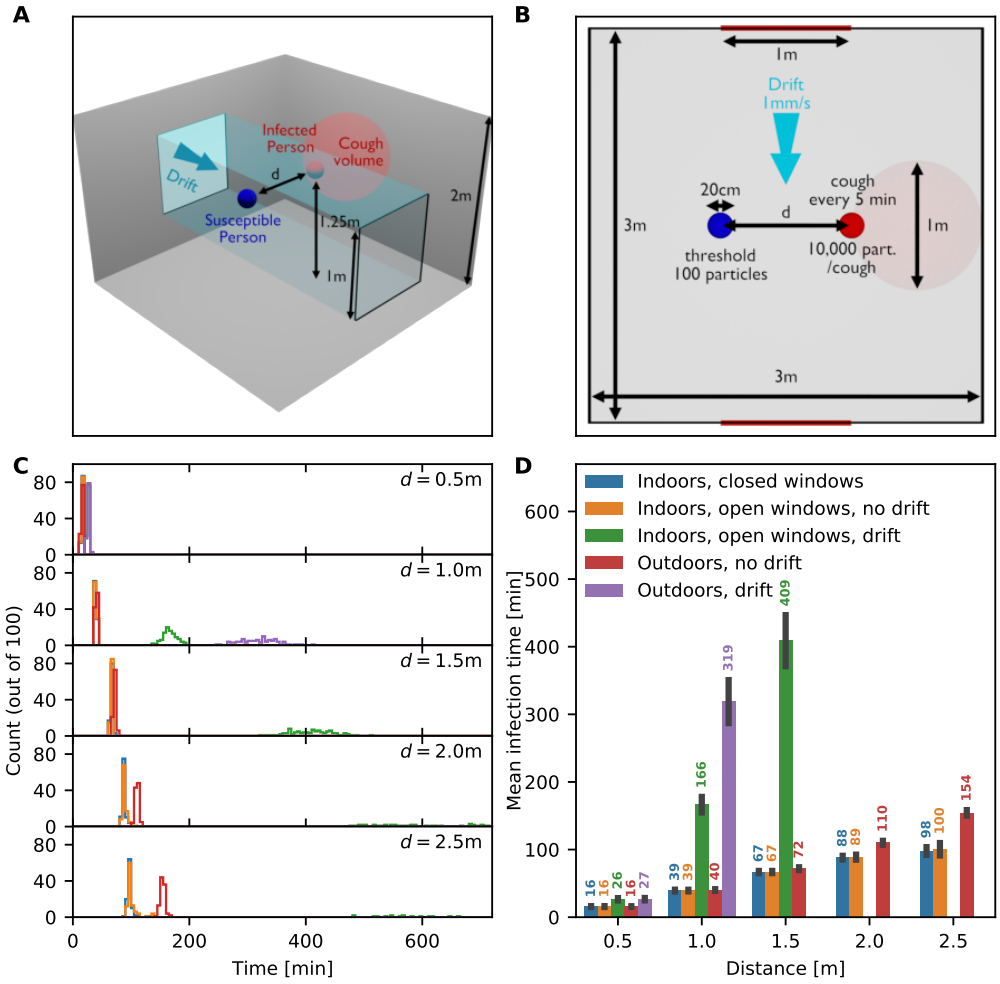

Figure 2. Infection times when an infected person is coughing once every 5 min. (a) 3D schematic representation of a closed room containing an infected (red) and a susceptible (blue) person separated by a variable distance d. The spherical volume in which 10^4 coughed particles are dispersed instantly is shaded red. As before, the room contains two windows which can be either open or closed with a possible drift between the windows. (b) Overhead view of (a). Room and window dimensions are displayed in the schematics. (c) Distribution of time of infection for distances $d = 0.5, 1, 1.5, 2$ and 2.5 m and the following scenarios: Indoors with windows closed (blue), indoors with open windows and no drift (orange), indoors with open windows and a drift (green), outdoors without drift (red), and outdoors with drift (purple). (d) Mean infection times for all scenarios. Missing bars indicate scenarios in which at least one realization had an infection time beyond 12 h. Error bars indicate the standard deviation of the time distribution.

2.3. *Coughing*

Next we evaluate the time to infection of a susceptible person using the same spatial configuration as before Figure 2a,b. Here, the infected person coughs every 5 min. We disregard the production of viral particles due to breathing here because the added particle influx is minuscule compared to the effects of coughing. The time to infection reduces drastically compared to breathing alone, as coughing leads to the instantaneous release of 10^4 particles in front of the infected person. Our results show that the distribution for the times of infection are peaked around the mean: at a distance of $d = 0.5$ m, the mean time to infection is 16 ± 1 min indoors and outdoors (regardless of the state of the windows) without a drift. This rises to 26 ± 2 min when there is a drift. At larger distances, a small drift more than triples the time to infection, which highlights the importance of distancing even when there is appropriate ventilation. Coughing at 30 s intervals shortens the time to infection by roughly a third (Figure 3). Note that we assumed that the infected person is facing away from the susceptible person when coughing (light red shaded region in Figure 1 a,b). As before, we do not show the mean time to infection if it is longer than 12 h.

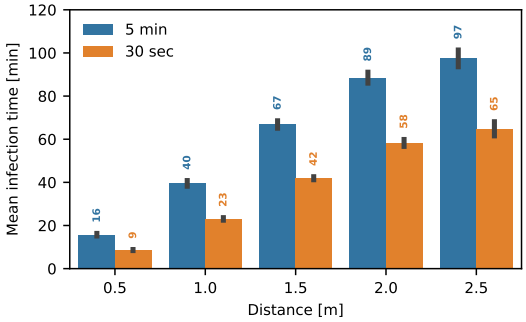

Figure 3. Influence of the cough interval. Mean time to infection for two different cough intervals, 5 min (blue) and 30 s (orange), and increasing distances d between the infected and susceptible persons. Error bars indicate the standard deviation of the time distribution.

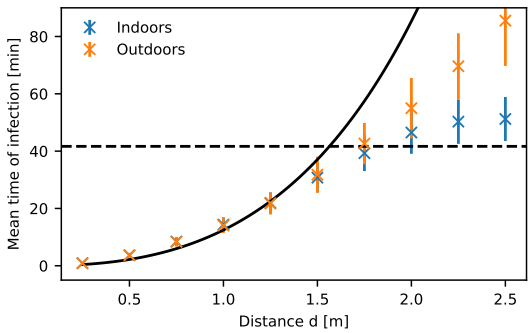

Figure 4. Mean infection time as a function of distance for a single cough. The mean infection time as a function of distance d from simulations (crosses) for the indoor case with windows closed (blue) and the outdoor case without any drift (orange) when the infected person is coughing once. Error bars indicate the standard deviation. The solid line shows τ_{inf} from Eq (4.12), together with the crossover time τ_c (dashed black line). Note that the threshold is set to two particles here (see Section 4.3).

We derived an analytical formula for the flux of viral particles being absorbed by the susceptible person Eq (4.9). Integrating this flux numerically and finding the time at which the cumulative number of absorbed particles crosses the infection threshold allows a direct comparison with our simulation results (Figure 4).

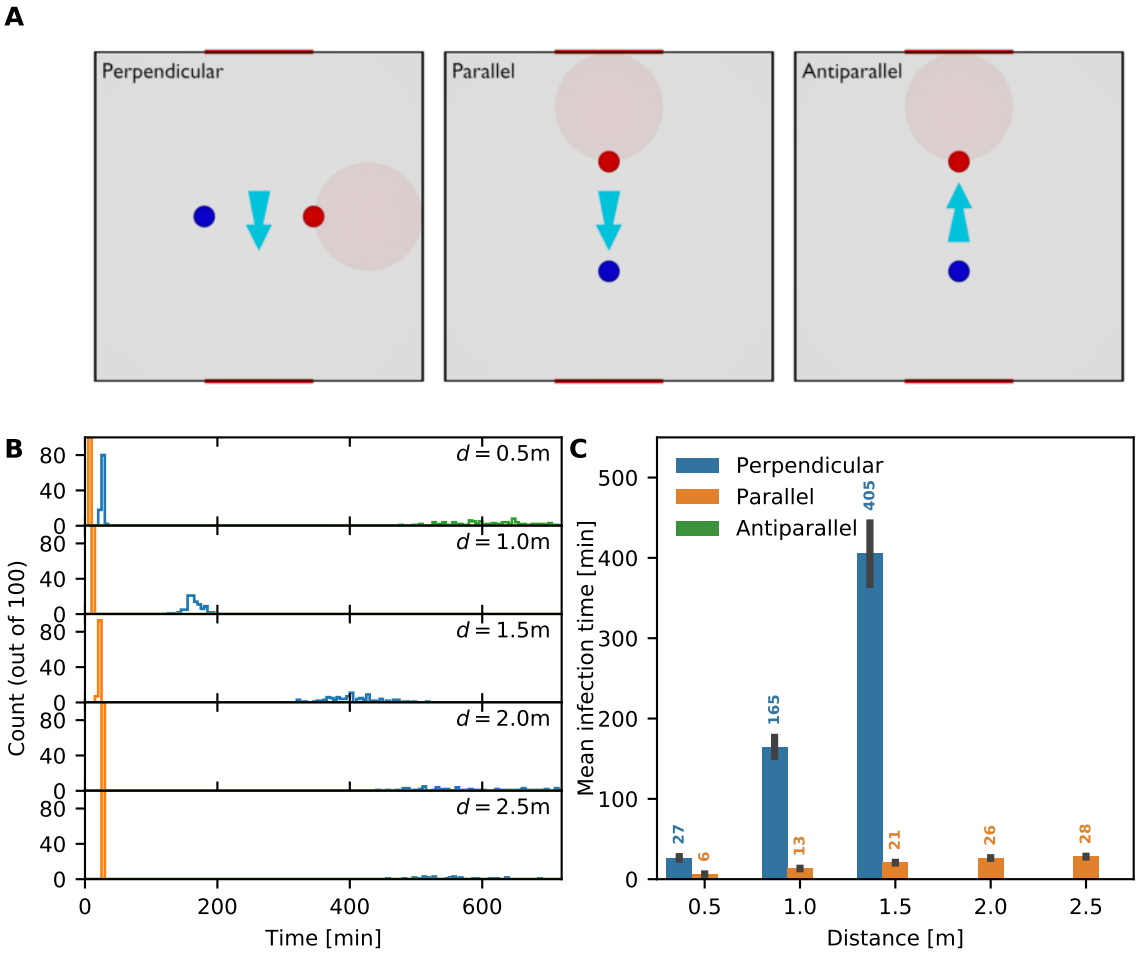

Figure 5. Influence of the direction of air movement. The mean time to infection as a function of distance and air movement direction for an infected person coughing in a room with open windows. (a) The light blue arrow indicates the direction of air movement/ventilation between the two windows. The direction of infection between the infected person (red circle) and the susceptible person (blue circle) can be perpendicular (left panel), parallel (middle panel) and antiparallel (right panel) to the direction of air movement. The shaded circle indicates the volume in which viral particles appear during coughing. (b) Distribution of time to infection for distances $d = 0.5, 1, 1.5, 2$ and 2.5 m and the scenarios: perpendicular (blue), parallel (orange) and antiparallel (green). (c) Mean infection time for the different scenarios. Missing bars indicate scenarios in which at least one realization had an infection time beyond 12 h. Error bars indicate the standard deviation of the time distribution.

We also looked at the importance of the direction of the air movement. Figure 2 shows the mean

time to infection when air moves perpendicular to the line connecting the infected and the susceptible person. When the drift is applied parallel to this line (i.e., particles are blown from the infected person towards the susceptible person), the mean time to infection is reduced such that infection occurs at the half-hour mark even at a distance of $d = 2.5$ m (Figure S1). When the wind direction is antiparallel, infection is not occurring within any reasonable time frame (Figure 5).

2.4. *Effect of wearing a mask*

Next, we evaluate the effect of a susceptible person wearing a mask on the time to infection. Surgical masks reduce the viral copy numbers in the fine diffusing fraction by a factor of 2.8 in viral aerosols [18]. We run similar simulations as above, where we model a mask by randomly counting only one in 2.8 particles that arrive at the susceptible person. When the infected person is breathing only (Figure 6), the mask increases the time to infection consistently by more than an hour for all distances. At $d = 0.5$ m, the time to infection more than doubles, from 95 ± 8 min to 200 ± 14 min. When the infected person is coughing, the effect of the mask is lessened, but still adds eight to 28 min depending on the distance.

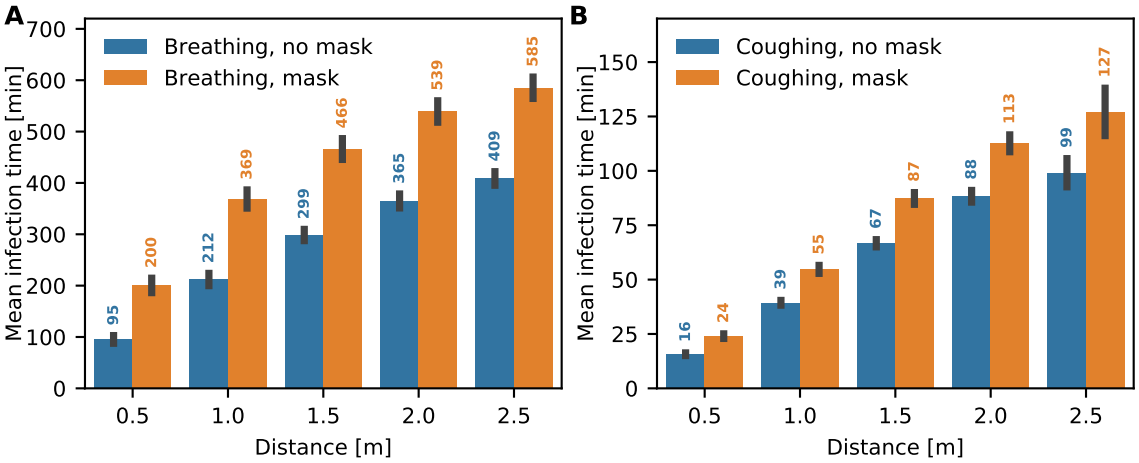

Figure 6. Effect of wearing a mask. (a) Mean infection times for various distances d = 0.5, 1, 1.5, 2 and 2.5 m (indoors with windows closed), with and without mask when the infected person is breathing only. The mask rejects on average 2.8 particles for every single particle it lets past. (b) Mean infection times for the same scenario as in (a), except that the infected person is coughing every 5 min. Error bars indicate the standard deviation of the time distribution.

2.5. *Parameter sensitivity*

Due to the large uncertainty in the value of key parameters such as the diffusion coefficient or the threshold of infection, we change their values and explore the consequence on the mean time of infection. Halving the threshold number of particles from 100 to 50 reduces the time to infection by only 4–13 min when the infected person is coughing, depending on the distance (Figure 7a; see Figure S3 for the breathing case). Increasing the threshold by an order of magnitude, from 100 to 1000 only roughly doubles the time to infection. Hence, the dependence of time to infection on

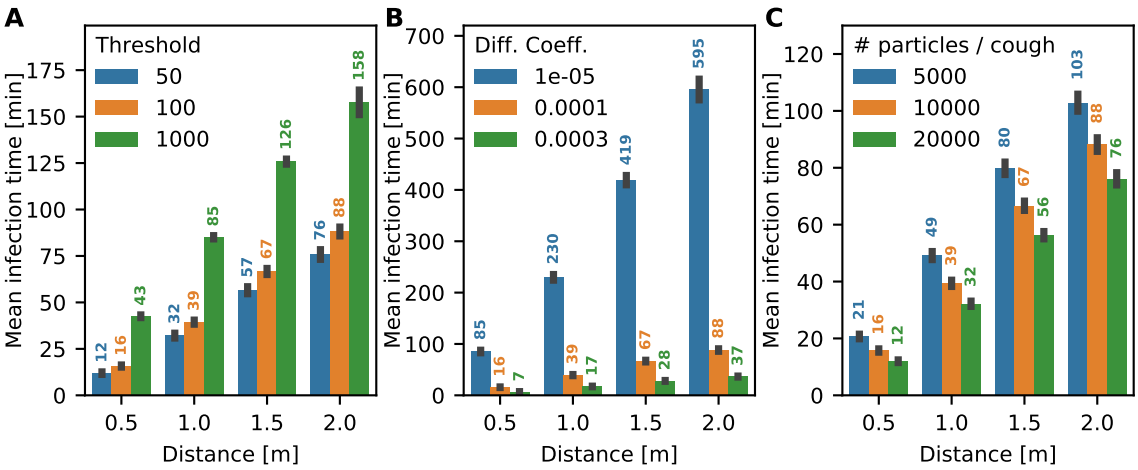

Figure 7. Sensitivity of the mean infection time to the threshold and diffusion coefficient. The mean infection time is estimated for an infected person coughing every 5 min in a room with windows closed. (a) Mean infection time for different values of the infection threshold count. (b) Influence of the diffusion coefficient. (c) Mean infection time versus the particle count contained in a cough. Error bars indicate the standard deviation of the time distribution.

the threshold is non-linear, as predicted by Eq (4.11) in the supplementary. Conversely, the value of diffusion coefficient has a significant effect: an increase from 10^{-5} m^2/s to 10^{-4} m^2/s decreases the infection time at $d = 1$ m from 230 min to 39 min. Finally, we vary the number of particles emitted during coughing from 5000 to 20000. At a distance of $d = 1$ m, this leads to a decrease of infection time from 49 min to 32 min. Therefore, wide variations in both the threshold number and the number of particles emitted during coughing have a comparatively small effect on the time to infection. In contrast, the diffusion determines the timescale, so its value does directly scale the time to infection. Even though these parameters are not known, the trends described above are still valid, if not the exact values of the time to infection.

3. Discussion

Here, we presented a model for airborne viral propagation based on diffusion of aerosols between an infectious and susceptible person [14, 17]. We focused on small aerosol particles ($< 5\ \mu$m) because they can deeply penetrate into the respiratory tract [28, 29], leading to a high probability of infection. A number of parameters used in our simulations, in particular the number of viral particles required for an infection, the number of viral particles emitted during breathing or coughing and the aerosol diffusion coefficient, are not well known and also would be difficult to estimate experimentally. We therefore based their values on other airborne viral illnesses (see Sections 4.1 and 4.2). To validate our results, we performed a series of parameter sensitivity studies that show that the trends we observe do not strongly depend on the exact parameter values (Figure 7).

The most striking result of the present study is the difference in time to infection between the cases when the infected person is breathing normally (e.g., during an asymptomatic infection) to when the infected person is coughing: A susceptible person needs to spend a considerable amount of time in close proximity to an infected person who is not coughing. This picture changes immediately when the

infected person is coughing (Table 1). While we did not look at speaking specifically, we can assume that if the infected person is talking (even if they are not coughing), the picture will be similar to the coughing case. According to the published literature, the accumulated number of aerosol particles emitted while speaking over a 5 min interval is similar to our assumption of 10^4 particles emitted all at once [2, 4, 11].

Table 1. Summary of the simulated time to infection at $d = 1$ m. The values shown are the time to infection in minutes at the CDC-recommended inter-person distance of 1 m for all cases we considered in our simulations.

	Breathing	Coughing
Indoors, closed windows	212 (369 with mask)	39 (55 with mask)
Indoors, open windows	220	39
Indoors, drift	> 12 h	166
Outdoors, no drift	248	40
Outdoors, drift	> 12 h	409

Coughing three times (once every five min) leads to infection in 15 min. Coughing every 30 s roughly halves this time, but does not shorten it by a factor of 10 as could be naively assumed. This is because we assume that the room is completely uncontaminated at the start of the simulation, without any viral particles present, and it takes time for aerosolized viral particles to disperse independently of the coughing frequency. Therefore, this is analogous to a situation where at time zero, the infected person enters the room and starts to cough. While we did not address the reverse situation where the susceptible person enters a room that already contains an infected person (and viral particles have had time to disperse), we can infer that, in this case, infection will occur much quicker. In a modeling study of influenza transmission, Atkinson and Wein found that a cough has a probability of roughly 25% to transmit the disease in a household setting [5, 29], which compares well to our findings.

Distance. Our results suggest that the time to infection increases roughly linearly with distance. Apart from coughing/breathing and ventilation, this is the parameter with the most influence on the infection time. Our results are consistent with the UK Scientific Advisory Group for Emergencies' report on the transmission risk of SARS-CoV-2, stating that a $1m$ separation carries 2–10 times the risk compared to a 2 m separation [8]. A recent meta-analysis of multiple different studies (also involving SARS-CoV-1 and MERS) found that the risk of infection approximately halved for every additional meter of separation [6].

Masks. We found that wearing a mask increases the time it takes to get infected when breathing only, which reinforces that consistent mask wearing reduces asymptomatic transmission (Figure 6, Table 1). It also increases the time to infection in the coughing case, although the effect is much smaller. Note that we only look at the small aerosol particle fraction, for which a mask is less efficient. We assume that the infectious person is coughing in a direction away from the susceptible person, which prevents spread via large droplets. Our results here are in line with recent findings that masks can stagger the pandemic over longer times, thereby preventing the saturation of intensive care units in hospitals [21].

Ventilation. We compared the time to infection indoors when windows are closed to when they are open (Figures 1 and 2; Table 1). In the absence of ventilation (i.e., a drift), the role of a window is to prevent the accumulation of viral particles in the room by creating a region that effectively absorbs particles. However, we find this is not enough to substantially affect the time to infection. If, in addition, there is ventilation (even a small drift is sufficient), the time to infection increases markedly. This assumes that this air movement is in any direction but from the infected to the susceptible person. In that case, the time to infection is reduced considerably (Figure S1). Therefore, we can conclude that ventilation is a good prevention strategy, but care must be taken about the direction of air movement.

Infection threshold number. The threshold number of particles required for an infection had only little effect on the infection time (Figure 7). This is due to waves of large numbers of particles being released with each cough event. In the regimes relevant for infection, the time to infection is then determined more by when the next wave of particles reaches the susceptible person rather than by how many are absorbed.

In summary, we believe that the present diffusion-based simulation method yields relevant insights into the relative effects of different scenarios, and also provides a good indication of the magnitude of the time to infection. However, we stress that since the simulation results are dependent on parameter values that are not well known and had to be inferred, the exact time to infection predicted by the simulations should not be taken at face value. Nevertheless, as we showed, the trends we present are valid and are in line with other findings in the literature and public guidance.

4. Methods

4.1. Model and simulations

The microscopic diffusion coefficient of aerosolized particles is estimated using the Einstein-Kolmogorov formula and is below 10^{-10} m^2/s. However, the dominant process in this case is not microscopic diffusion, but turbulent diffusion, where the effective diffusivity is increased to $D = 10^{-4}$ m^2/s . To simulate the spread of aerosolized viral particles, we use Brownian motion. The position $\vec{X}_i$ of each particle i satisfies the Smoluchowski limit of the Langevin equation [24]

$$d\vec{X}_i = \vec{F}(\vec{X}_i)dt + \sqrt{2D}d\vec{W}_i, \tag{4.1}$$

where $\vec{F}(\vec{x})$ specifies a possible drift due to air movement (open windows in the indoor case, or wind in the outdoor case), D is the diffusion coefficient of the aerosolized particle, W is a Wiener process. We discretize this equation using the Euler-Maruyama algorithm (forward time stepping) using custom-written code.

Interaction with various surfaces is accounted for by various boundary conditions: In the indoors case, particles are reflected by walls, floor and ceiling, placed at the $x, y, z = 0$ m and $x, y = 3$ m and $z = 2$ m positions. Windows are located at the $y = 0$ m and $y = 3$ m walls, with the extents $0.5\text{m} < z < 1.5$ m and $1\text{ m} < x < 2$ m. Note that we disregard particle deposition at surfaces.

If windows are open, a particle's trajectory is terminated once it crosses the window boundary (i.e., windows represent absorbing boundaries). In the outdoors case, only the floor at $z = 0$ m is reflecting, and we restrict our computational domain to a spherical domain with a radius of 10 m. The optional

drift is applied with $\vec{F}([x, y, z])\vec{e}_y$ either throughout the domain in the outdoors case or limited to the region 0.5 m $< z <$ 1.5 m and 1 m $< x <$ 2 m in the indoors case (i.e., directly between the windows). While the drift is likely to be stronger outdoors than when two windows are open indoors depending on weather and wind, we nevertheless opted to input the same drift strength in both cases. This was done to be able to have comparable scenarios, but will likely underestimate the mean infection time outdoors.

In the case of breathing, the infected person is modelled by a point source that randomly emits particles with an average rate of 10 particles per minute. In the case of coughing to include effects from jets and puffs, the source of particles is a spherical volume directly in front of the infected person's head, facing away from the susceptible person and of 1 m diameter, in which 10^4 particles are randomly placed every 5 min (in the case of coughing).

The susceptible person is modelled as an absorbing spherical surface of 10 cm radius, a distance d away from the infected person. When a threshold number of particles has been absorbed by the sphere, the time of this event is recorded as the time of infection and the simulation terminated. A summary of all simulation parameters can be found in Table 2.

Table 2. Parameter summary. The values of all parameters used throughout all our simulations, unless explicitly stated otherwise in the text. Particle emission rate and coughing parameters are only used in the breathing-only and coughing cases, respectively.

All cases	
Effective turbulent diffusivity D	10^{-4} m^2 / s
Inter-person distance d	0.5 – 2.5 m
Room size (indoors only) $W \times L \times H$	$3 \times 2 \times 2$ m
Window size $W \times H$	1×1 m
Absorbing sphere diameter	20 cm
Drift	0 or 1 mm / s
Infection threshold T	100 particles
Maximum simulation time	12 h
Breathing only	
Particle emission rate	10 particles / min
Coughing	
Number of particles per cough	10^4
Cough interval	5 min
Cough volume diameter	1 m

4.2. Limitations of the method

Our approach, while well-suited to the simulation of the spreading of aerosolized particles, also has limitations when applied to the spread of viral infections:

- **Small versus large droplets:** We only consider the spreading of small particles/droplets. Larger droplets (above 5 μm) are not well described by the diffusion approach. However, these particles

will also reasonably quickly drift to the ground due to gravity. Therefore, they would modify our results only for small distances between susceptible and infected persons, decreasing the time to infection.

- **Diffusion coefficient:** The diffusion coefficient of the particles is determined by their size. While aerosolized particles have a distribution of sizes, we make the simplification that particles have a fixed size and hence a fixed diffusion coefficient. Since the diffusion coefficient essentially sets the timescale of infection, the value of the diffusion coefficient influences the time to infection. Therefore, the absolute values of the mean time to infection directly depend on the diffusion coefficient, but the qualitative trends (such as the effect of wearing a mask or ventilation) are independent of it. Since the diffusion coefficient becomes larger for smaller particles, the infection dynamics is dominated by the smallest infectious particles. We chose the size (and hence the diffusion coefficient) to be consistent with aerosol droplets containing one viral particle each on average.
- **Threshold for infection and coughing:** Some parameters are not well-known or need to be inferred from other airborne viral illnesses such as influenza. The threshold number of particles required for an infection is not known for SARS-CoV-2, but medical experts estimate it to be between hundreds and thousands of particles [22, 23]. We decided to use a threshold number of 100 particles, the lowest reasonable number. This ensures that our model under-estimates rather than over-estimates the mean time to infection. Furthermore, the mean time to infection is surprisingly insensitive to the exact threshold (Figure 7a). The average number of particles emitted during coughing is also not well-known, but similar to the threshold number, the time to infection is not strongly dependent to the exact value (Figure 7c).
- **Walls:** Here, walls, the floor, and the ceiling are reflective for droplets, but they could also simply stick to surfaces. Removing them would lead to less droplet load, making the mean time to infection longer. However, comparing our indoors and outdoors simulations, this effect is small. We disregard any furniture, or the bodies of the infected and susceptible people, which would likely only have a small effect on the mean time to infection. This is because the threshold is reached by the fastest set of particles that moves directly toward the respiratory tracks.
- **Drift:** In the scenarios that include a drift, we assumed a small drift strength representing light air movement. Stronger air movement will more strongly affect the mean time to infection, but the direction of this effect depends on the exact setting (see supplementary Figure S1). We assumed the same drift strength for our indoor and outdoor scenarios. Depending on wind and weather, and for a perpendicular wind direction, this likely understates the drift in the outdoor case; hence, our results likely underestimate the mean infection time. In the case of a parallel wind, this depends strongly on its direction (parallel versus antiparallel, see Figure S1).

4.3. Analytical formula for the viral particle flux

We use the theory of diffusion to estimate the flux of droplets to the nose entrance of a susceptible person: after N_0 droplets are instantaneously released following breathing, sneezing, or coughing, they diffuse into the surrounding air. We neglect any surrounding surfaces such as floors and walls and, as above, assume that infection occurs when the number of droplets reaches a given threshold T. The

spatial distribution of droplets satisfies the diffusion equation

$$\begin{aligned}\frac{\partial p(\boldsymbol{x},t\,|\,\boldsymbol{x}_0)}{\partial t} &= D\Delta p(\boldsymbol{x},t\,|\,\boldsymbol{x}_0) \quad \text{for } \boldsymbol{x},\boldsymbol{x}_0 \in \mathbb{R}^3,\\ p_0(\boldsymbol{x},t\,|\,\boldsymbol{y}) &= p_0(\boldsymbol{x},t\,|\,\boldsymbol{x}_0) = N_0\delta(\boldsymbol{x}-\boldsymbol{x}_0) \quad \text{for } \boldsymbol{x},\boldsymbol{x}_0 \in \mathbb{R}^3\\ p_0(\boldsymbol{x},t\,|\,\boldsymbol{y}) &= 0 \quad \text{for } \boldsymbol{x} \in \partial\Omega_a\\ p(\boldsymbol{x},t\,|\,\boldsymbol{x}_0) &\to 0 \quad \text{for } \boldsymbol{x} \to \infty,\end{aligned} \tag{4.2}$$

where $\boldsymbol{x}_0$ is the position of the source (i.e., the infected person). The flux of droplets on an absorbing surface near the face ($\partial\Omega_a$) of a susceptible person is given by

$$\Phi(t) = -D\int_{\partial\Omega_a} \frac{\partial p}{\partial \boldsymbol{n}}(\boldsymbol{x},t\,|\,\boldsymbol{x}_0)dS_{\boldsymbol{x}} \tag{4.3}$$

and the cumulative number of particles absorbed is

$$F(t) = \int_0^t \Phi(s)ds. \tag{4.4}$$

When the source (i.e., the infectious person) is at $\boldsymbol{x}$ and the target (i.e., the susceptible person) is located at position $\boldsymbol{y}$, the distribution is given by

$$p(\boldsymbol{x},t\,|\,\boldsymbol{y}) = \frac{N_0}{(4\pi Dt)^{3/2}}\exp\left(-\frac{|\boldsymbol{x}-\boldsymbol{y}|^2}{4Dt}\right). \tag{4.5}$$

By neglecting the variation of the flux on the surface $\partial\Omega_a$ when the distance between the two faces is large, $\delta = |\boldsymbol{x}-\boldsymbol{y}| \gg 1$, the flux can be approximated by

$$\Phi(t) \approx \delta\frac{N_0}{(4\pi Dt)^{3/2}(2t)}|\partial\Omega_a|\exp\left(-\frac{\delta^2}{4Dt}\right). \tag{4.6}$$

Figure 8 shows the absorbed flux of viral particles as a function of time for different distances. Note the sharp spike in the flux for small distances, which is smoothened for larger distances.

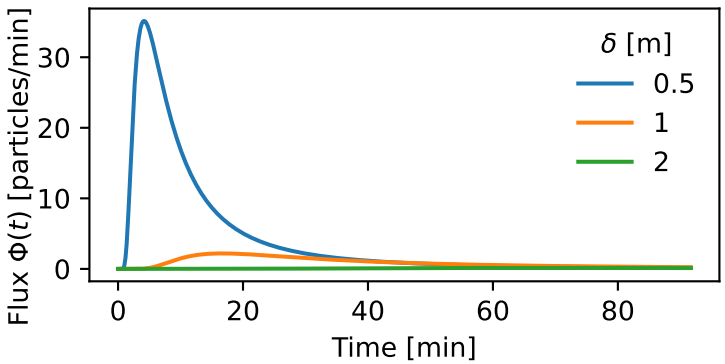

Figure 8. Analytical absorbed flux for a single cough at $t = 0$. Flux of particles absorbed by the susceptible person for different inter-person distances δ from Eq (4.3). The infected person coughs once, releasing $10,000$ particles instantaneously at $t = 0$. Here, the diffusion coefficient is set to $D = 10^{-4}\text{m}^2/\text{s}$.

The number of inhaled particles over time is then

$$F(t) = \delta|\partial\Omega_a| \int_0^t \frac{N_0}{(4\pi D s)^{3/2}(2s)} \exp\left(-\frac{\delta^2}{4Ds}\right) ds = \frac{N_0|\partial\Omega_a|}{2\pi^{3/2}} \frac{1}{\delta^2} g(\frac{4Dt}{\delta^2}), \tag{4.7}$$

where $g(x) = \int_0^x \frac{1}{s^{5/2}} \exp\left(-\frac{1}{s}\right) ds$. Note that for short times $\frac{4Dt}{\delta^2} \ll 1$, $g(\frac{4Dt}{\delta^2}) \approx \frac{\delta}{\sqrt{4Dt}} \exp\left(-\frac{\delta^2}{4Dt}\right)$ and thus

$$F\left(t \ll \frac{\delta^2}{4D}\right) = \frac{N_0|\partial\Omega_a|}{2\pi^{3/2}} \frac{1}{\delta\sqrt{4Dt}} \exp\left(-\frac{\delta^2}{4Dt}\right). \tag{4.8}$$

For long times, g approaches a constant given by $g(\frac{4Dt}{\delta^2} \to \infty) = \sqrt{\pi}/2$ (Figure S4). The relevant time scale here is $\tau_c = \frac{\delta^2}{4D}$, which at $\delta = 1$ m and with $D = 10^{-4}$ m^2/s, $\tau_c = 2500$ s ≈ 42 min. The time of infection τ_{inf} is achieved when the total number of inhaled particle reaches the threshold T_{inf}:

$$\tau_{inf} = \inf\{t > 0 \quad \text{s.t.} \quad F(t) = T\}. \tag{4.9}$$

Note that the probability of an infection occurring earlier than τ_{inf} can be defined by

$$Pr\{t < \tau_{inf}\} = \frac{F(t)}{F(T)} = \frac{g(\frac{4Dt}{\delta^2})}{g(\frac{4DT}{\delta^2})}. \tag{4.10}$$

When infection occurs in the time regime before τ_c, we can invert relation (4.8) to get $\frac{T\delta^2 2\pi^{3/2}}{N_0|\partial\Omega_a|} = \frac{\delta}{\sqrt{4Dt}} \exp\left(-\frac{\delta^2}{4Dt}\right)$ leading to

$$\frac{\delta^2}{4Dt} = W_0\left(2\left[\frac{T\delta^2 2\pi^{3/2}}{N_0|\partial\Omega_a|}\right]^2\right), \tag{4.11}$$

where W_0 is the positive branch of the Lambert function. With $W_0(x) = \ln(x) - \ln(\ln x) + o(1)$, it can be approximated as

$$\tau_{inf} \approx \frac{\delta^2}{D}\left[\ln\left(\frac{T\delta^2(2\pi)^{3/2}}{N_0|\partial\Omega_a|}\right)\right]^{-1} \tag{4.12}$$

Interestingly, relation Eq (4.12) shows that the infection time depends weakly on the threshold (as the reciprocal of the logarithm). Expression (4.12) matches well with data from stochastic simulations for infection times $\tau_{inf} < \tau_c$ for a single cough (Figure 4). Note that we changed the threshold to 2 particles for this, to push the infection time below the τ_c threshold for small distances.

4.4. Distribution of the time to infection for periodic particle release

We can extend the previous analysis for repetitive expulsion of particles (i.e., coughing). At the point source, we periodically inject a load of particles. In this case, we can define the elementary injection time Δt_{inj} (Δt_{breath} or Δt_{cough}) leading to the following condition at the source:

$$p_0(\boldsymbol{x}, t\,|\,\boldsymbol{y}) = \sum_{k>0} N_0 \delta(\boldsymbol{x} - y)\delta(t - k\Delta t_{inj}), \tag{4.13}$$

where N_0 is the number of viral particles expelled by the infected person during each period. Using the relations 4.2 and 4.3, we obtain the total flux due to breathing only,

$$\Phi_{breath/cough}(t) \approx \delta \sum_{k>0} \frac{N_0}{(4\pi D(t-t_k))^{3/2}(2(t-t_k))} |\partial\Omega_a| \exp\left(-\frac{\delta^2}{4D(t-t_k)}\right), \tag{4.14}$$

where $t_k = k\Delta_{breath}$ in the case of breathing and $t_k = k\Delta_{cough}$ in the case of coughing. Figure 9 shows the case of periodic expulsion of viral particles, such as breathing and coughing every 5 min (expelling 10000 particles each time) outdoors. Note the non-linear oscillations in particle flux, which are dampened by smaller values of the diffusion coefficient (Figure 9b). After the infectious person leaves the scene, the aerosol concentration decays exponentially.

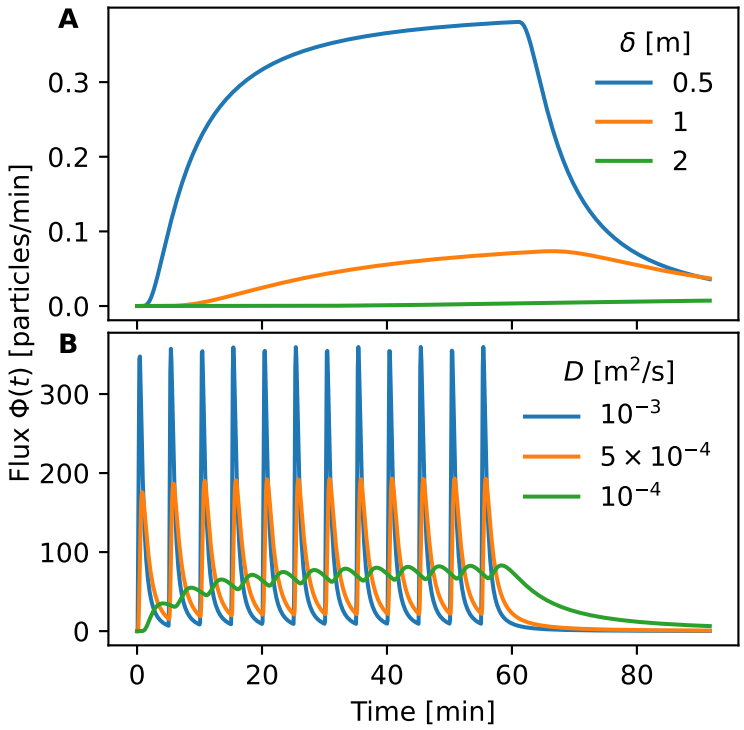

Figure 9. Analytical absorbed flux for a periodic source of viral particles. Flux of particles absorbed by the susceptible person from Eq (4.14) when the infected person (a) breathes out 10 particles per minute (as a function of the inter-person distance δ and $D = 10^{-4}\text{m}^2/\text{s}$); and (b) coughs every 5 min, releasing 10,000 particles with each cough (for different values of the diffusion coefficient D and $\delta = 0.5$ m). After 60 min, the infected person leaves the room, which leads to an exponential decay of the flux over time.

In the combined case, when both breathing and coughing are considered, the total flux is simply the sum of the two:

$$\Phi_{total}(t, \delta) = \Phi_{breathing}(t) + \Phi_{Cough}(t). \tag{4.15}$$

The time to infection is the first time that the total number of particles reaches the threshold T_{inf}

$$\tau_{inf} = \inf\{t > 0 \quad \text{s.t.} \quad \Phi_{total}(t) = T\}. \tag{4.16}$$

Finally, we can define the probability of infection at time t for distance δ for a viral load threshold T as

$$Pr\{t, \delta|T\} = \frac{\Phi_{Total}(t, \delta)}{\Phi_{Total}(T, \delta)}. \tag{4.17}$$

In the fast-load-release approximation (i.e., coughing repeatedly at a high frequency), and by considering that most of the viral particles are expelled at the maximum of the coughing event, we can obtain a linear regime of accumulation:

$$\Phi_{Cough}(t) \approx \frac{3N_0}{8\pi\delta^2}|\partial\Omega_a|t. \tag{4.18}$$

Use of AI tools declaration

The authors declare that they have not used Artificial Intelligence (AI) tools in the creation of this article.

Conflict of interest

The authors declare that there are no conflicts of interest.

References

1. R. H. Alford, J. A. Kasel, P. J. Gerone, V. Knight, Human influenza resulting from aerosol inhalation, *Proceedings of the Society for Experimental Biology and Medicine*, **122** (1966), 800–804. https://doi.org/10.3181/00379727-122-31255
2. M. Alsved, A. Matamis, R. Bohlin, M. Richter, P. E. Bengtsson, C. J. Fraenkel, et al., Exhaled respiratory particles during singing and talking, *Aerosol Sci Tech*, **54** (2020), 1245–1248. https://doi.org/10.1080/02786826.2020.1812502
3. P. Anfinrud, C. E. Bax, V. Stadnytskyi, A. Bax, *Could Sars-Cov-2 be transmitted via speech droplets ?*, MedRxiv, [Preprint], (2020), [cited 2024 April 04]. Available from: https://doi.org/10.1101/2020.04.02.20051177
4. S. Asadi, A. S. Wexler, C. D. Cappa, S. Barreda, N. M. Bouvier, W. D. Ristenpart, Aerosol emission and superemission during human speech increase with voice loudness, *Sci. Rep.*, **9** (2019), 1–10. https://doi.org/10.1038/s41598-019-38808-z
5. M. P. Atkinson, L. M. Wein, Quantifying the routes of transmission for pandemic influenza, *Bull. Math. Biol.*, **70** (2008), 820–867. https://doi.org/10.1007/s11538-007-9281-2
6. D. K. Chu, E. A. Akl, S. Duda, K. Solo, S. Yaacoub, H. J. Schünemann, et al., Physical distancing, face masks, and eye protection to prevent person-to-person transmission of Sars-Cov-2 and Covid-19: a systematic review and meta-analysis, *The Lancet*, **395** (2020), 1973–1987. https://doi.org/10.1016/S0140-6736(20)31142-9
7. B. J. Cowling, D. K. Ip, V. J. Fang, P. Suntarattiwong, S. J. Olsen, J. Levy, et al., Aerosol transmission is an important mode of influenza a virus spread, *Nat Commun*, **4** (2013), 1–6. https://doi.org/10.1038/ncomms2922

8. EMG (Environmental and Modelling Group), Transmission of SARS-CoV-2 and Mitigating Measures. Scientific Advisory Group for Emergencies, 2020. Available from: https://www.gov.uk/government/publications/transmission-of-sars-cov-2-and-mitigating-measures-update-4-june-2020

9. P. Fabian, J. J. McDevitt, W. H. DeHaan, R. O. P. Fung, B. J. Cowling, K. H. Chan, et al., Influenza virus in human exhaled breath: An observational study, *Plos One*, **3** (2008), 1–6. https://doi.org/10.1371/journal.pone.0002691

10. J. Gawn, M. Clayton, C. Makison, B. Crook, Evaluating the protection afforded by surgical masks against influenza bioaerosols, Health and Safety Executive, 2008. https://api.semanticscholar.org/CorpusID:36385715

11. F. K. Gregson, N. A. Watson, C. M. Orton, A. E. Haddrell, L. P. McCarthy, T. J. Finnie, et al., Comparing aerosol concentrations and particle size distributions generated by singing, speaking and breathing, *Aerosol Sci Tech*, **55** (2021), 681–691. https://doi.org/10.1080/02786826.2021.1883544

12. K. M. Gustin, J. M. Katz, T. M. Tumpey, T. R. Maines, Comparison of the levels of infectious virus in respirable aerosols exhaled by ferrets infected with influenza viruses exhibiting diverse transmissibility phenotypes, *J. Virol.*, **87** (2013), 7864–7873. https://doi.org/10.1128/jvi.00719-13

13. N. H. Leung, D. K. Chu, E. Y. Shiu, K. H. Chan, J. J. McDevitt, B. J. Hau, et al., Respiratory virus shedding in exhaled breath and efficacy of face masks, *Nat. Med.*, **26** (2020), 676–680. https://doi.org/10.1038/s41591-020-0843-2

14. Q. Li, X. Guan, P. Wu, X. Wang, L. Zhou, Y. Tong, et al., Early transmission dynamics in wuhan, china, of novel coronavirus–infected pneumonia, *N Engl J Med*, **382** (2020), 1199–1207. https://doi/full/10.1056/NEJMOa2001316

15. W. G. Lindsley, F. M. Blachere, K. A. Davis, T. A. Pearce, M. A. Fisher, R. Khakoo, et al., Distribution of airborne influenza virus and respiratory syncytial virus in an urgent care medical clinic, *Clin. Infect. Dis.*, **50** (2010), 693–698. https://doi.org/10.1086/650457

16. W. G. Lindsley, T. A. Pearce, J. B. Hudnall, K. A. Davis, S. M. Davis, M. A. Fisher, et al., Quantity and size distribution of cough-generated aerosol particles produced by influenza patients during and after illness, *J Occup Environ Hyg*, **9** (2012), 443–449. https://doi.org/10.1080/15459624.2012.684582

17. Y. Liu, Z. Ning, Y. Chen, M. Guo, Y. Liu, N. K. Gali, et al., Aerodynamic analysis of Sars-Cov-2 in two wuhan hospitals, *Nature*, **582** (2020), 557–560. https://doi.org/10.1038/s41586-020-2271-3

18. D. K. Milton, M. P. Fabian, B. J. Cowling, M. L. Grantham, J. J. McDevitt, Influenza virus aerosols in human exhaled breath: particle size, culturability, and effect of surgical masks, *Plos Pathog*, **9** (2013), e1003205. https://doi.org/10.1371/journal.ppat.1003205

19. N. Nikitin, E. Petrova, E. Trifonova, O. Karpova, Influenza virus aerosols in the air and their infectiousness, *Adv. Virus. Res.*, **2014**. https://doi.org/10.1155/2014/859090

20. H. Qian, T. Miao, L. Li, X. Zheng, D. Luo, Y. Li, Indoor transmission of Sars-Cov-2, *Indoor Air*, **31** (2020), 639–645. https://doi.org/10.1111/ina.12766

21. J. Reingruber, A. Papale, D. Holcman, *Monitoring and predicting Sars-Cov-2 epidemic in france after deconfinement using a multiscale and age-dependent model*, MedRxiv, [Preprint], (2020), [cited 2024 April 04]. Available from: https://doi.org/10.1101/2020.05.15.20099465

22. Roundups and Rapid Reactions, Expert reaction to questions about covid-19 and viral load. Science Media Centre, 2020. Available from https://www.sciencemediacentre.org/expert-reaction-to-questions-about-covid-19-and-viral-load.

23. S. Samuel, Why you're unlikely to get the coronavirus from runners or cyclists, VOX, 2020. Available from: https://www.vox.com/future-perfect/2020/4/24/21233226/coronavirus-runners-cyclists-airborne-infectious-dose

24. Z. Schuss, *Theory and applications of stochastic processes: an analytical approach*, Berlin: Springer Science & Business Media, 2009.

25. J. H. Seinfeld, S. N. Pandis, *Atmospheric chemistry and physics: from air pollution to climate change*, New York: John Wiley & Sons, 2016.

26. V. Stadnytskyi, C. E. Bax, A. Bax, P. Anfinrud, The airborne lifetime of small speech droplets and their potential importance in Sars-Cov-2 transmission, *PNAS*, **117** (2020), 11875–11877. https://doi.org/10.1073/pnas.2006874117

27. J. W. Tang, W. P. Bahnfleth, P. M. Bluyssen, G. Buonanno, J. L. Jimenez, J. Kurnitski, et al., Dismantling myths on the airborne transmission of severe acute respiratory syndrome coronavirus-2 (Sars-Cov-2), *J. Hosp. Infect.*, **110** (2021), 89–96. https://doi.org/10.1016/j.jhin.2020.12.022

28. R. Tellier, Review of aerosol transmission of influenza a virus, *Emerg Infect Dis.*, **12** (2006), 1657–1662. https://doi.org/10.3201%2Feid1211.060426

29. R. Tellier, Aerosol transmission of influenza a virus: a review of new studies, *J. R. Soc. Interface.*, **6** (2009), S783–S790. https://doi.org/10.1098/rsif.2009.0302.focus

30. R. Tellier, Y. Li, B. J. Cowling, J. W. Tang, Recognition of aerosol transmission of infectious agents: a commentary, *BMC Infect Dis*, **19** (2019), 1–9. https://doi.org/10.1186/s12879-019-3707-y

31. J. Wang, G. Du, Covid-19 may transmit through aerosol, *Ir J Med Sci*, **189** (2020), 1143–1144. https://doi.org/10.1007/s11845-020-02218-2

32. C. Ward, M. Dempsey, C. Ring, R. Kempson, L. Zhang, D. Gor, et al., Design and performance testing of quantitative real time pcr assays for influenza a and b viral load measurement, *J Clin Virol*, **29** (2004), 179–188. https://doi.org/10.1016/S1386-6532(03)00122-7

33. J. Yan, M. Grantham, J. Pantelic, P. J. B. De Mesquita, B. Albert, F. Liu, et al., Infectious virus in exhaled breath of symptomatic seasonal influenza cases from a college community, *PNAS*, **115** (2018), 1081–1086. https://doi.org/10.1073/pnas.1716561115

Supplementary

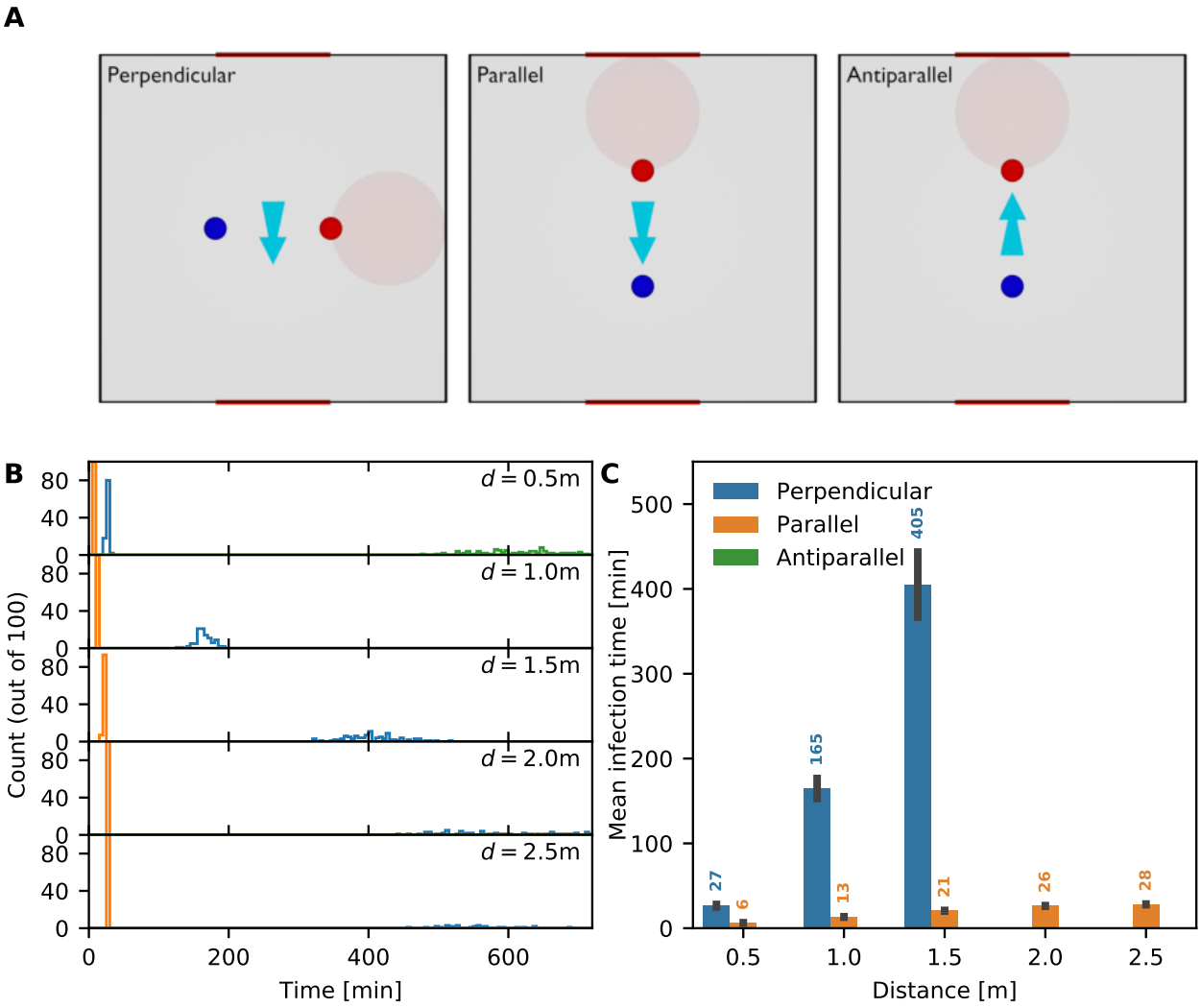

Figure S1. Influence of the direction of air movement. The mean time to infection as a function of distance and air movement direction for an infected person coughing in a room with open windows. (a) The light-blue arrow indicates the direction of air movement/ventilation between the two windows. The direction of infection between the infected person (red circle) and the susceptible person (blue circle) can be perpendicular (left panel), parallel (middle panel) and antiparallel (right panel) to the direction of air movement. The shaded circle indicates the volume in which viral particles appear during coughing. (b) Distribution of time to infection for distances $d = 0.5, 1, 1.5, 2$, and 2.5 m and the scenarios: perpendicular (blue), parallel (orange), and antiparallel (green). (c) Mean infection time for the different scenarios. Missing bars indicate scenarios in which at least one realization had an infection time beyond 12 h. Error bars indicate the standard deviation of the time distribution.

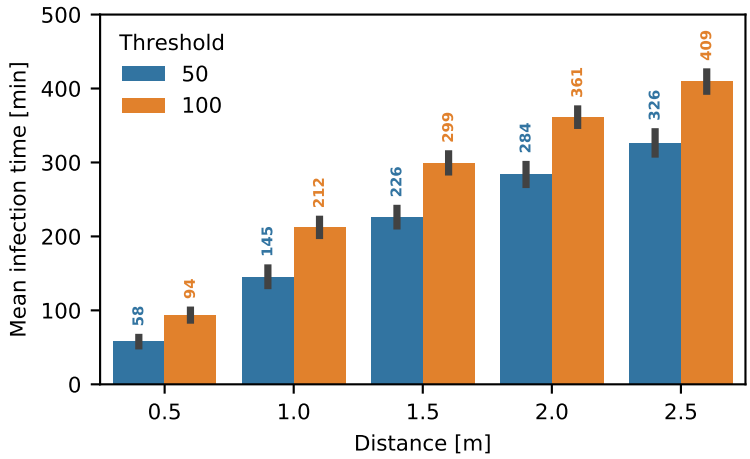

Figure S2. Influence of the threshold number of particles required for infection in the breathing case. Mean time to infection for two different values of the threshold, 50 (blue) and 100 absorbed particles. Error bars indicate the standard deviation of the time distribution.

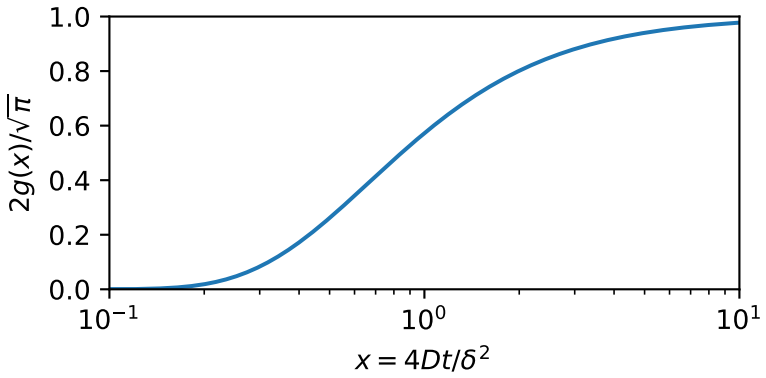

Figure S3. Plot of function $2g(x)/\sqrt{\pi}$. Normalized visualisation of the function g defined in Eq (4.7) in the main text. For $x \to \infty$, g approaches a constant value of $\sqrt{\pi}/2$.